

How to apply importance-sampling techniques to simulations of optical systems

C. J. McKinstrie and P. J. Winzer

Bell Laboratories, Lucent Technologies, Holmdel, New Jersey 07733

Abstract

This report contains a tutorial introduction to the method of importance sampling. The use of this method is illustrated for simulations of the noise-induced energy jitter of return-to-zero pulses in optical communication systems.

When one rolls a die, the probability of it stopping with a particular number face-up is $1/6$. To measure such a probability experimentally and accurately, one must roll the die many more than 6 times. With this fact in mind, consider the design of optical communication systems. A common way to evaluate system prototypes is to measure (in computer simulations or laboratory experiments) the distance over which they can transmit information with bit-error-ratios of order 10^{-9} (without forward error correction). Even with current computers, it is impractical to simulate pulse transmission many more than 10^9 times.

One can use importance-sampling techniques to circumvent this difficulty. Put simply, bit errors are caused by large system perturbations (deviations from ideal behavior) that occur infrequently. When one makes importance-sampled simulations of system performance one biases them in such a (controlled) way that these large perturbations occur more often than they should. Because they occur often, one can measure their statistics accurately. Subsequently, one adjusts the simulation results to remove their artificial bias. In this way one obtains results that are both unbiased and accurate.

Pioneering importance-sampled simulations of phase noise in an optical system were made by Foschini and Vannuci [1]. Recently, importance-sampled simulations of polarization-mode dispersion were made by Biondini *et al.* [2]. Importance-sampling methods were reviewed comprehensively by Smith *et al.* [3] and ways to combine data from different importance-sampled simulations were discussed by Veach [4]. In this report we make no attempt to duplicate their discussions. Rather, we show by example how to apply importance-sampling techniques to optical systems.

It is instructive to consider the die example quantitatively. Each roll of an unbiased die is a trial, in which the probability of a successful outcome $p = 1/6$ and the value associated with a successful outcome (the weight with which a successful outcome is counted) $w = 1$. For each trial the expected value of the outcome is pw and the variance is $w^2p(1-p)$. Suppose that an unbiased die is rolled n_1 times and let f_1 be the measured 1-frequency (the number of 1s divided by the number of rolls). Then the expected value of the 1-frequency $E(f_1) = 1/6$. By adding n_1 terms of magnitude $5/36$ and dividing the result by n_1^2 one finds that the variance $V(f_1) = 5/36n_1$: To measure the 1-frequency with an accuracy of 1% (to conduct an experiment for which the standard deviation of the 1-frequency is 1% of the expected

value) one would have to roll the die 5×10^4 times. This would be a time-consuming task.

If the 5- and 6-frequencies were of no interest one could bias the die by marking the 5- and 6-faces with 1s. Since this change would increase the probability of rolling a 1 ($p = 3/6 = 1/2$), one should count each successful roll with reduced weight ($w = 1/3$). Suppose that this biased die is rolled n_2 times and let f_2 be the measured (weighted) 1-frequency. Then the expected value $E(f_2) = 1/6$, as required, and the variance $V(f_2) = 1/36n_2$: By causing the desired event to occur more often than it would naturally, one is able to measure its probability more accurately, or with fewer rolls. (For rare events that occur in applications, the performance improvements are much larger than the factor of 5 associated with this example.) Of course, the price one pays for this increase in accuracy is the loss of information about the 5- and 6-frequencies.

If these frequencies were of limited, but finite, interest, one could combine the measurements made with each die separately. If one were to weight the two measurements equally, by defining the combined 1-frequency $f = (f_1 + f_2)/2$, one would find that $E(f) = 1/6$ and $V(f) = 5/144n_1 + 1/144n_2$: The accuracy of the combined measurement is limited by the less-accurate individual measurement (the one with the larger variance coefficient or the one made with fewer rolls). One should weight the individual measurements in proportion to the numbers of rolls used to make them, and in inverse proportion to their variance coefficients. Let $f = c_1f_1 + c_2f_2$, where the condition $c_1 + c_2 = 1$ ensures that $E(f) = 1/6$. Then a short calculation shows that the optimal values of c_1 and c_2 are $n_1/(n_1 + 5n_2)$ and $5n_2/(n_1 + 5n_2)$, respectively, in which case the minimal variance $V(f) = 5/36(n_1 + 5n_2)$. For the case in which $n_1 = n_2 = n/2$, where n is the total number of rolls, $V(f) = 5/108n$.

In this dice example simple formulas for the individual variances exist, which allow one to determine the optimal weight coefficients precisely. However, in applications such formulas might be complicated or unknown. Consequently, a different method is required. An effective method, which is called the balance heuristic [4], is to weight each successful outcome (roll of either die) equally. In this method, if the unbiased die is rolled n_1 times and the biased die is rolled n_2 times, the combined probability of rolling a 1 is $(n_1 + 3n_2)/6(n_1 + n_2)$. To ensure that the expected value of the combined measurement is $1/6$, each successful roll (of either die) should be counted with weight $w = (n_1 + n_2)/(n_1 + 3n_2)$. By adding n_1 contributions

of magnitude $w^2 p_1(1 - p_1)$ and n_2 contributions of magnitude $w^2 p_2(1 - p_2)$, and dividing the result by $(n_1 + n_2)^2$, one finds that the combined variance is $(5n_1 + 9n_2)/36(n_1 + 3n_2)^2$. For the case in which $n_1 = n_2 = n/2$ the combined variance is $7/144n$, which is only 5% larger than the minimal variance of the preceding paragraph. Thus, one should weight each outcome in inverse proportion to its combined probability.

Now consider the noise-induced energy (amplitude) jitter of a return-to-zero (RZ) pulse. Provided that the pulse energy e is greater than the noise energy in the surrounding bit slot, it evolves according to the stochastic ordinary differential equation (ODE)

$$d_z e = (g - \alpha)e + r, \quad (1)$$

where $g(z)$ is the amplifier gain rate, α is the fiber loss rate and $r(z)$ is the rate at which the energy is changed by amplifier noise [5, 6]. This random rate of change is quantified by the equations $\langle r(z) \rangle = 0$ and $\langle r(z)r(z') \rangle = (2n_{\text{sp}}h\nu g e)\delta(z - z')$, where $\langle \rangle$ denotes an ensemble average, n_{sp} is the spontaneous-emission factor (1.1–1.3) and $h\nu$ is the photon energy. Equation (1) is valid for any isolated pulse and an arbitrary combination of distributed and lumped amplification.

For definiteness, consider a 10 Gb/s system with uniformly-distributed amplification ($g = \alpha$), in which $\alpha = 0.21$ dB/Km, $\beta = -0.30$ ps²/Km ($D = 0.38$ ps/Km-nm) and $\gamma = 1.7$ /Km-W. Then a soliton with a full-width at half-maximum of 30 ps has an energy of 21 fJ (time-averaged power of 0.21 mW). If the system length $l = 10$ Mm the output noise power in both polarizations, in a frequency bandwidth of 12 GHz (wavelength bandwidth of 0.1 nm), is 1.7 μ W: The (optical) signal-to-noise ratio is 21 dB. Systems with nonuniformly-distributed or lumped amplification produce the same noise power in shorter distances.

For uniformly-distributed amplification Eq. (1) can be rewritten in the canonical form

$$dx = x^{1/2} dy, \quad (2)$$

where $x = e/e_0$ is the energy, normalized to the equilibrium energy (in the absence of noise), and y is a Wiener process (Gaussian random variable) with $\langle y \rangle = 0$ and $\langle y^2 \rangle = \sigma_s^2 z$, where the normalized source-strength $\sigma_s^2 = 2n_{\text{sp}}h\nu g/e_0$. In the linear regime the multiplicative factor $x^{1/2} \approx 1$, from which it follows that $x \approx 1 + y$: The probability-density function (PDF) of the output energies is Gaussian, with mean 1 and variance $\sigma_s^2 z$. (From a logical

standpoint the PDF of the non-negative quantity x cannot be exactly Gaussian, because, if it were, the probability of $x < 0$ would be finite for all $z > 0$. From a practical standpoint this inconsistency is tolerable if the probability of $x < 0$ is exponentially small for system lengths of interest.) For the aforementioned system the output variance $\sigma_s^2 l = 6.6 \times 10^{-3}$ (which is of order 10^{-2}) and the output deviation is 8.1×10^{-2} (which is of order 10^{-1}). In the nonlinear regime the factor $x^{1/2}$ modifies the tails of the PDF significantly. For reference, the analytical solution of Eq. (2) has the PDF

$$P(x) \approx \frac{\cosh(mx^{1/2}/v) \exp[-(m^2 + x)/2v]}{(2\pi xv)^{1/2}}, \quad (3)$$

where $m = 1 - \sigma_s^2 z/8$ and $v = \sigma_s^2 z/4$ [7].

Equation (2) and solution (3) model energy jitter in a (continuous) system with uniformly-distributed amplification. We simulated a (discrete) system with $n_i = 100$ lumped amplifiers. Between the amplifiers the energy x did not change. At the i th amplifier the energy was changed (kicked) by the random amount δy_i , where the properties $\langle \delta y_i \rangle = 0$ and $\langle \delta y_i \delta y_j \rangle = 10^{-4} \delta_{ij}$ ensured that $\langle (\sum_{i=1}^{n_i} \delta y_i)^2 \rangle = 10^{-2}$: The discrete system had the same characteristics as the continuous system. The output energies were assigned to energy bins of (common) width 0.02 and each bin probability p_j was defined to be the number of pulses whose energies fell within the bin boundaries (bin count) divided by the total number of pulses. (Since probabilities cannot be measured by finite numbers of trials, these quantities should be called the relative frequencies associated with the bins. We use the term probabilities as an abbreviation for the correct term.) To facilitate comparisons to the analytical PDF (3), the simulation probabilities were defined to be the bin probabilities divided by the bin width. In these (direct) simulations the occurrence of each output energy was counted with unit weight.

The PDF associated with an ensemble of 10^6 pulses is displayed in Fig. 1. Although the simulation results agree well with Eq. (3) near the peak of the PDF, they do not even begin to sample the tail of the PDF. On a 1-GHz PC these simulations, which are based on Eq. (2), take a few minutes. Simulating the transmission of many more than 10^9 pulses would take many days. Realistic simulations, which are based on the nonlinear Schroedinger equation, would take even longer.

To probe the tails of the PDF one must make large energy perturbations occur more

often than they would naturally. One way to achieve this goal is to increase the standard deviation of the energy kicks. Let q_0 denote the (common) unbiased kick distribution, with deviation $\sigma_0 = 10^{-2}$, and q denote the (common) biased kick distribution, with deviation $\sigma > \sigma_0$. Then, at the i th amplifier the probability that the energy is kicked by the amount δy_i is increased by the factor $q(\delta y_i)/q_0(\delta y_i)$. Since the kicks at all the amplifiers are biased, the output energy occurs with a probability that is larger than its natural probability by the total factor $f_t = \prod_{i=1}^{n_i} q(\delta y_i)/q_0(\delta y_i)$, which depends on the full kick sequence $(\delta y_1, \delta y_2, \dots, \delta y_{n_i})$. One can remove this bias by counting the output energy with reduced weight: One increments the appropriate bin probability by $1/f_t$, rather than 1. All other aspects of data counting remain the same. For reference, the probability factor $1/f_t$ is called the likelihood ratio.

The PDF associated with an ensemble of 10^6 pulses is displayed in Fig. 2 for the case in which $\sigma = 1.2\sigma_0$. The results of these (importance-sampled) simulations differ from the previous results in two ways. First, they do probe the tail of the PDF. Although the simulations reproduce the shape of the analytical PDF, the simulation probabilities are not accurate because the number of data points that sample the tail of the PDF is still small. Second, by causing large kicks to happen more often, one causes small kicks to happen less often. Consequently, the body (peak) of the PDF is not reproduced accurately. This deficiency prevents one from increasing σ until the tail of the PDF is sampled accurately.

Another way to achieve the stated goal is to change the (common) mean of the kick distributions. If the mean kick μ is positive (negative) the energy drifts toward larger (smaller) values. The distributions associated with 3 ensembles of 3×10^5 pulses are displayed in Fig. 3 for cases in which $\sigma = \sigma_0$, and $\mu = -3 \times 10^{-3}$, 0 and 3×10^{-3} . These values produce data sets with mean energies of -0.3 , 0.0 and 0.3 , respectively. Although the simulation distributions are inaccurate for energies that are far from their mean energies (because the bin counts are low), they are accurate near their mean energies. It only remains to combine the individual distributions to produce a composite distribution that is accurate for the entire domain of interest.

One way to combine the individual distributions is to weight their bin probabilities equally (which is equivalent to combining the data sets before sorting the output energies and the associated probability factors into bins). Let p_{jk} be the j th bin probability associated with

the k th data set (which was produced by kick distributions with mean μ_k). For each j , if the individual bin probabilities p_{jk} were all zero the combined bin probability p_j was defined to be zero and if some of the p_{jk} were nonzero p_j was defined to be their average. The results of this procedure are shown in Fig. 4. Although the composite distribution does cover the domain of interest, it is inaccurate near the boundaries of the sample spaces. Combining the individual distributions with equal weight allows the bodies of the distributions (which have high bin counts) to be polluted by the tails of neighboring distributions (which have low bin counts).

The dice example suggests that it is better to weight the bin probabilities according to the associated bin counts. For each j , if the individual bin counts b_{jk} were all zero the combined bin probability p_j was defined to be zero and if some of the bin counts were nonzero p_j was defined to be $\sum_{k=1}^{n_k} b_{jk} p_{jk} / \sum_{k=1}^{n_k} b_{jk}$. The results of this procedure are shown in Fig. 5. The composite distribution covers, and is accurate throughout, the domain of interest. This *ad-hoc* procedure allows one to combine bin probabilities generated at different times, without recourse to the data sets on which they were based.

Although the *ad-hoc* method works, it is not the balance heuristic. Suppose that the kick sequence $(\delta y_1, \delta y_2, \dots, \delta y_{n_i})$ occurs during the first simulation, which is made using the biased distribution q_1 (with mean μ_1). Then the associated probability factor $f_{t1} = \prod_{i=1}^{n_i} q_1(\delta y_i) / q_0(\delta y_i)$. Were the same sequence to occur during the k th simulation, the associated probability factor would be f_{tk} , which depends on the biased distribution q_k . If the simulations involve the same number of pulses, the combined probability factor $f_t = \sum_{k=1}^{n_k} f_{tk} / n_k$. (It is easy to generalize this formula.) When we made the individual simulations and sorted the output energies and the individual probability factors into bins, we also sorted the combined probability factors into a separate set of bins, which was common to all the simulations. The results of this procedure are shown in Fig. 6. The balance-heuristic method works well.

In summary, we showed by example how to apply importance sampling techniques to simulations of optical communication systems. These techniques are easy to apply and increase significantly the accuracy with which rare events can be simulated.

We acknowledge useful discussions with D. Chizhik, G. Foschini, R. Moore and J. Salz.

Postscript: Independent simulations of energy jitter were made recently by Moore *et al.* [Opt. Lett. **28**, 105 (2003)], who showed that the predictions of the energy equation (1) are consistent with the results of simulations based on the nonlinear Schroedinger equation.

References

- [1] G. J. Foschini and G. Vannuci, “Characterizing filtered light waves corrupted by phase noise,” IEEE Trans. Inform. Theory **34**, 1437–1448 (1988).
- [2] G. Biondini, W. L. Kath and C. R. Menyuk, “Importance sampling for polarization-mode dispersion,” IEEE Photon. Technol. Lett. **14**, 310–312 (2002).
- [3] P. J. Smith, M. Shafi and H. Gao, “Quick simulation: a review of importance sampling techniques in communication systems,” IEEE J. Sel. Areas in Commun. **15**, 597–613 (1997) and references therein.
- [4] E. Veach, “Robust Monte Carlo methods for light transport simulation,” Ph.D. thesis, Stanford University (1997).
- [5] C. J. McKinstrie and C. Xie, “Phase jitter in single-channel soliton systems with constant dispersion,” IEEE J. Sel. Top. Quantum Electron. **8**, 616–625 (2002) and references therein.
- [6] C. J. McKinstrie, C. Xie and C. Xu, “Effects of cross-phase modulation on phase jitter in soliton systems with constant dispersion.” Opt. Lett. **28**, 604-606 (2003).
- [7] This approximate solution was discovered during a collaboration with T. I. Lakoba. Its derivation will be described elsewhere.

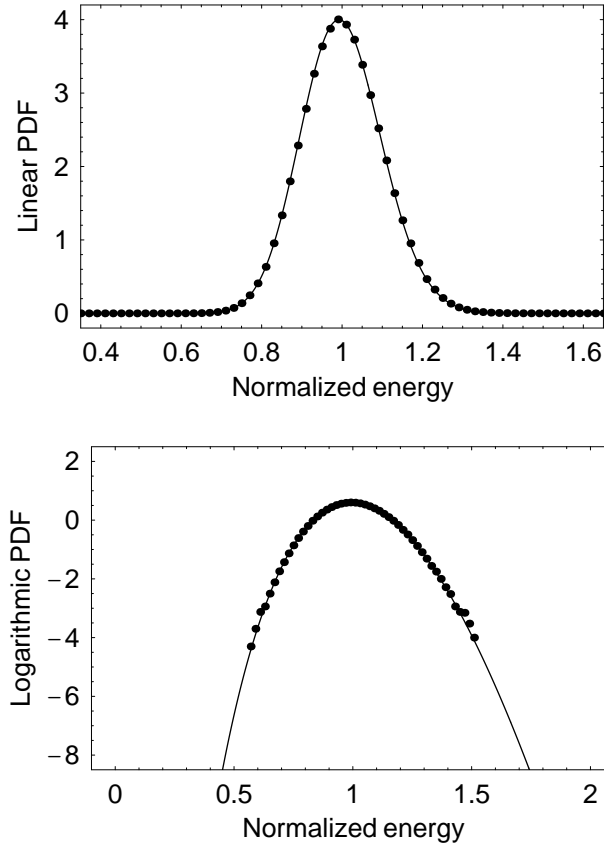


Figure 1: Probability distribution function of the (normalized) output energies obtained by solving Eq. (2) analytically (curve) and numerically, for an ensemble of 10^6 pulses (dots). The standard deviation of the energy kicks was 10^{-2} .

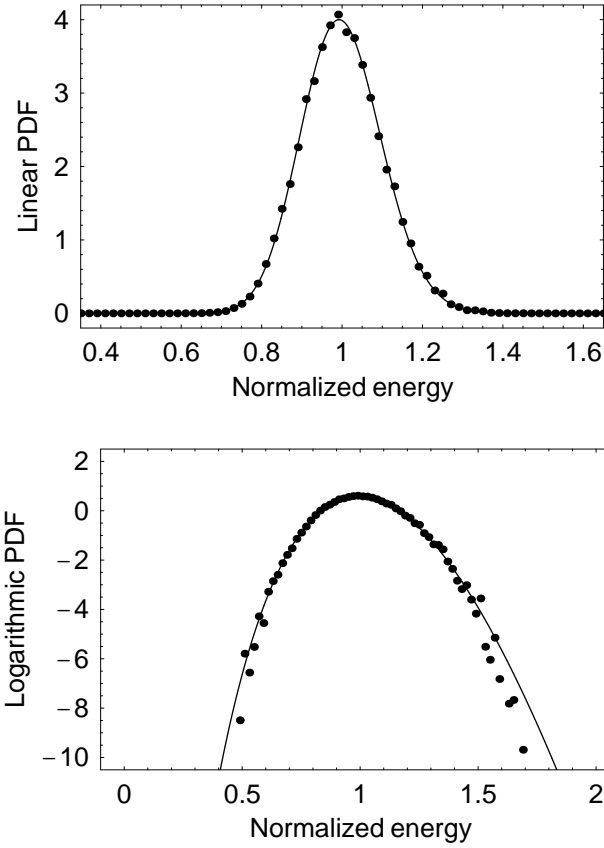


Figure 2: Probability distribution function of the (normalized) output energies obtained by solving Eq. (2) analytically (curve) and numerically, for an ensemble of 10^6 pulses (dots). The standard deviation of the energy kicks was 1.2×10^{-2} .

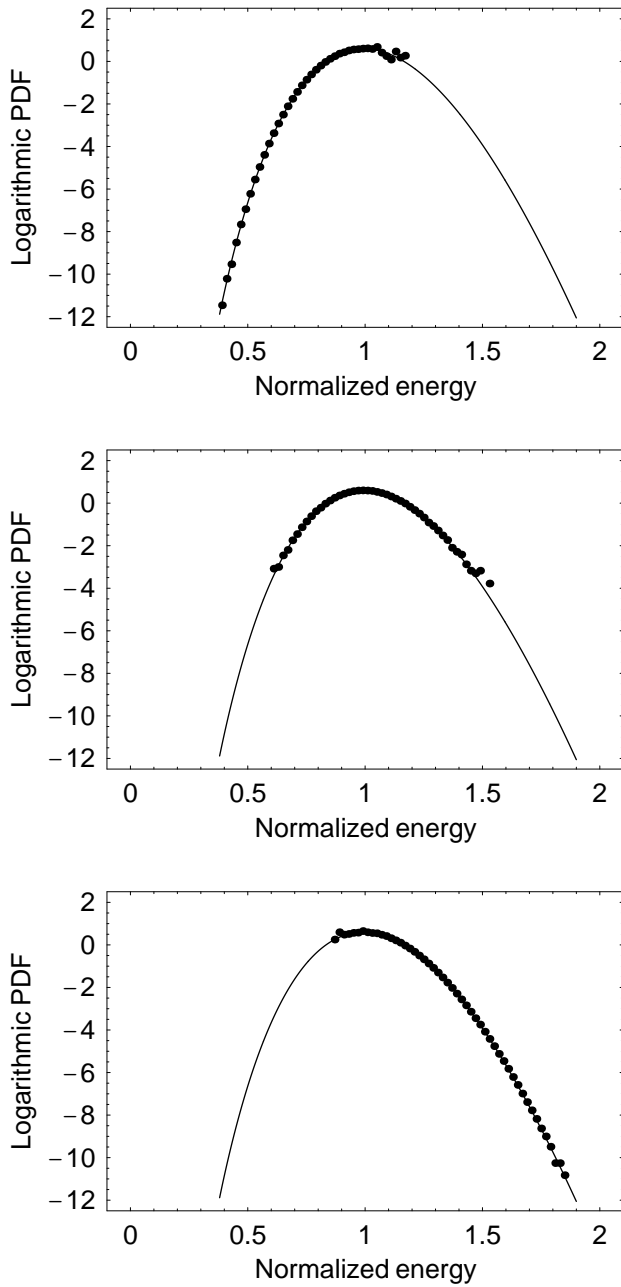


Figure 3: Probability distribution functions of the (normalized) output energies obtained by solving Eq. (2) analytically (curve) and numerically, for 3 ensembles of 3×10^5 pulses (dots). For each ensemble the standard deviation of the energy kicks was 10^{-2} . The mean energy kicks were -3×10^{-3} , 0 and 3×10^{-3} .

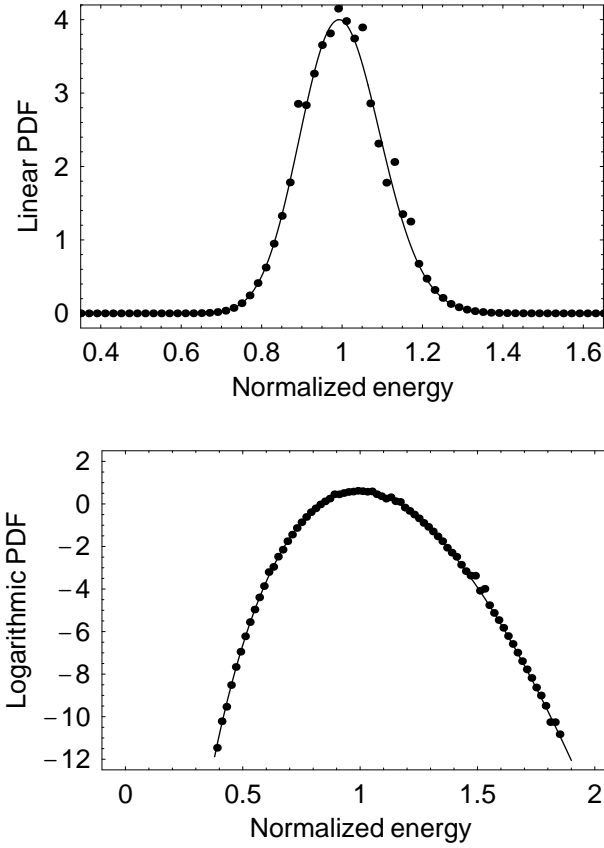


Figure 4: Probability distribution function of the (normalized) output energies obtained by solving Eq. (2) analytically (curve) and numerically, for 3 ensembles of 3×10^5 pulses (dots). For each ensemble the standard deviation of the energy kicks was 10^{-2} . The mean energy kicks were -3×10^{-3} , 0 and 3×10^{-3} . The 3 sets of bin probabilities were combined without weighting.

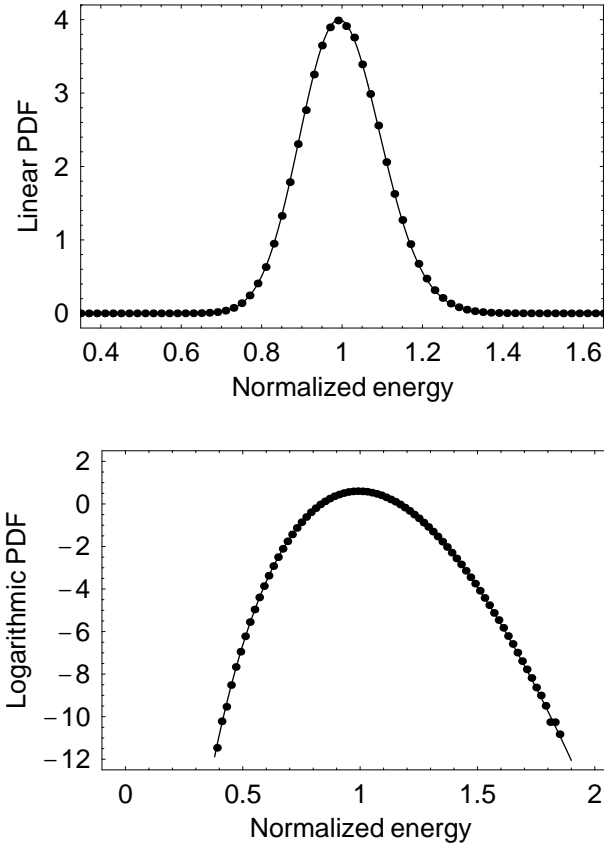


Figure 5: Probability distribution function of the (normalized) output energies obtained by solving Eq. (2) analytically (curve) and numerically, for 3 ensembles of 3×10^5 pulses (dots). For each ensemble the standard deviation of the energy kicks was 10^{-2} . The mean energy kicks were -3×10^{-3} , 0 and 3×10^{-3} . When the 3 sets of bin probabilities were combined, they were weighted according to the associated bin counts.

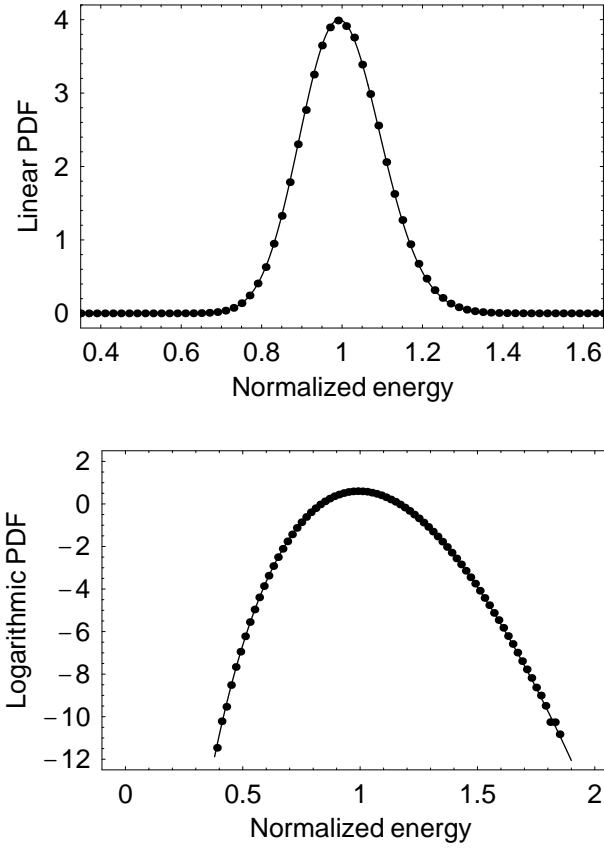


Figure 6: Probability distribution function of the (normalized) output energies obtained by solving Eq. (2) analytically (curve) and numerically, for 3 ensembles of 3×10^5 pulses (dots). For each ensemble the standard deviation of the energy kicks was 10^{-2} . The mean energy kicks were -3×10^{-3} , 0 and 3×10^{-3} . When the 3 data sets were combined, the data were weighted according to the combined probability factors.